IUST
Iran University of Science and Technology

Iranian Journal of Electrical and Electronic Engineering

Journal Homepage: ijeee.iust.ac.ir

Compact Two-Port MIMO Antenna with High Isolation for UWB Applications

Shivanand Konade*(C.A.), Manoj Dongre*

Abstract: The proposed research presents a two-port compact Multiple Input Multiple Output (MIMO) antenna for Ultra-Wide Band (UWB) applications. The designed antenna has two identical radiators and has an overall dimension of 20 × 44.1 × 1.6mm^3 on a FR4 substrate. The designed antenna is fed by a 50-microstrip line. Extended F-shaped stubs are introduced in the shared ground plane of the proposed antenna to produce high isolation between the MIMO antenna elements. Extended F-shaped stubs are introduced in the ground plane to produce multiple resonance and high isolation between the radiating elements. The antenna offers good impedance matching in the UWB band. The proposed antenna has lower isolation < -25 dB and Envelope Correlation Coefficient (ECC) < 0.015 from 3.1 to 10.6 GHz. Antenna parameters are evaluated in term of return loss, ECC, Diversity Gain (DG), gain, Total active reflection coefficient (TRAC) radiation pattern and isolation. The proposed antenna is tested and fabricated. However, obtained results are good agreement which make suitable for UWB wearable applications.

Keywords: Compact, ECC, Isolation, MIMO, and UWB antenna.

1 Introduction

IN 2002, the Federal Communication Commission (FCC) allocated the unlicensed UWB frequency band from 3.1 to 10.6 GHz [1]. Over the past decade, UWB technology has received a lot of attention and tremendous progress due to increasing data rates and channel capacities. However, UWB technology suffers from multipath fading effect and has poor indoor coverage [2]. To address this issue, a MIMO antenna has been designed on the transmitter and receiver side for UWB applications. MIMO antennas allow communication systems to improve communication efficiency, enhance coverage, and increase channel capacity [3]. UWB MIMO antenna must be small in design and easy install in portable devices. The enhanced features of MIMO UWB antennas such as high data rate and exclusion from interference make it a perfect candidate for wearable applications. To meet these objectives, many techniques for MIMO antennas have been presented in the literature [4-5]. Weak isolation between the elements of MIMO antennas occurs when they are arranged in a small area. The objective of present research is to design a MIMO antenna with reduced dimensions and improved isolation. For UWB applications, different antenna forms have been suggested [6-8]. MIMO antennas are made up of many antennas that must have strong isolation and be compact in size. Various approaches, such as Electromagnetic Band Gap (EBG), Complementary Split Ring Resonator (SRR), Defected Ground Structure (DGS), Decoupling Stubs and Neutralisation Line, have been employed to produce high isolation and small dimensions [9-18]. In [9], antenna elements are perpendicular to each other to produce high isolation and polarization diversity. To reduce mutual coupling, a parasitic T-shaped strip is used between the radiating components as a decoupling structure. The impedance bandwidth of antenna is from 3.1 to 11.08 GHz and Lower than - 15 dB mutual coupling exists between

Iranian Journal of Electrical & Electronic Engineering, 2024.
Paper first received 31 October 2023 and accepted 15 June 2024.
* The authors are with the Electronics and Telecommunication Department, Ramrao Adik Institution of Technology, Dr.D.Y. Patil University Nerul, Navi Mumbai.
E-mail: shivanand.konade@dypatil.edu.
Corresponding Author: Shivanand Konade.

ports. Size of antenna is 38.5 × 38.5 mm^2. In [10], Two antennas are placed orthogonal to each other. To reduce electromagnetic interference and improve isolation metamaterial unit structure is used. Isolation of an antenna is less than 25, impedance bandwidth is 65.5% and overall dimension of substrate is 40 × 80 mm^2. Shunt short-circuited stubs and three inter digital edge coupled microstrip lines, are used in feedline in [11], to obtain frequency cut-off and improve selectivity. The impedance bandwidth of an antenna is from 3.1-10.6 GHz. The size of antenna is 68 × 35 mm^2. A multi-branch stub with square monopole antenna is constructed in [12] to decrease mutual coupling. The antenna dimension is 40 × 20 mm^2. Resonating frequency is from 3-11 GHZ and isolation is less than -15 dB. In [13], F-shaped stub is used in ground plane to achieve high isolation. Overall size of antenna is 50 × 30 mm^2 with impedance bandwidth is from 2.5–14.5 GHz. In [30], a hexagonal ring components MIMO antenna is presented. Arc-shaped stub is used to achieve good isolation on 45 × 25mm^2 substrate. Antenna isolation is greater than -15 dB, and the impedance bandwidth from 3.1-12 GHz. UWB-MIMO antenna with GSM band is presented in [15]. Antenna design on 36 × 45 mm^2 substrate with frequency band from 3.01-12.5 GHz. The isolation is less than -20 dB. In [16], T-shaped stub is used to reduce mutual coupling of an antenna. The overall length of antenna is 24 × 32 mm^2 with 3.1–12.5 GHz frequency band. T-shaped stub is used to minimize the mutual coupling is presented in [17]. The overall dimension of an antenna is 26 × 28 mm^2. In [18], circular shape MIMO antenna is presented. Decoupling structures are used in the top and bottom layers of the substrate to reduce mutual coupling. Size of antenna is 40 × 40 mm^2 with operating frequency is from 3.1–11 GHz. The planar microstrip array antenna with a 4 × 4 modified Butler matrix is presented [21]. An effective method to suppress mutual coupling between two substrate integrated waveguide (SIW) slot antenna arrays is presented [22]. The antenna structures in [9-15] have large dimensions. In [16-17], antenna size is small, but isolation is low. A compact two-port MIMO antenna for UWB applications is proposed. The MIMO antenna is made up of two identical radiating components arranged in the shape of a right triangle. To achieve high isolation, extended F shapes of stubs are used in the ground plane. S_{12} < -25dB is obtained over the frequency range 3.1-10.6 GHz. The antenna has a stable radiation pattern with an ECC of 0.01. The antenna is smaller in size than the most recent reported antennas.

2 Antenna Geometry and Design Theory

The structure of the MIMO antenna constructed on a 20 × 44.1 × 1.6 mm^3 substrate is illustrated in Figure 1. The effect of with and without stubs in the ground plane are discussed in this section. The proposed antenna is built on a FR4 substrate with a dielectric constant of εr = 4.4 and a loss tangent of 0.02. The antenna is made up of two right triangle radiating elements connected by a 50 Ω microstrip line. The centres of the radiating elements are separated by 26.5 mm. The antenna's structure must be small enough to accommodate the space between the two patches with distances between them of about λ0/2 (λ0 is the free space wavelength), in case of the distance between the patches is larger than λ0/2, the mutual coupling is already small. Mutual coupling among neighbouring antenna elements can take place when antenna elements are close to each other, this effect can reduce MIMO channel capacity. The feed line length and width are 6 and 3 mm, respectively. The ground plane width is the same as the width of the antenna, and its length is 4.47 mm. F type stubs are utilised in the ground plane to increase impedance bandwidth and isolation. The optimized antenna parameter is shown in table 1.

We have added design equation, relationship between the distance the antennas and impact of the distance between the fed points on input impedance are added in the revised manuscripts.

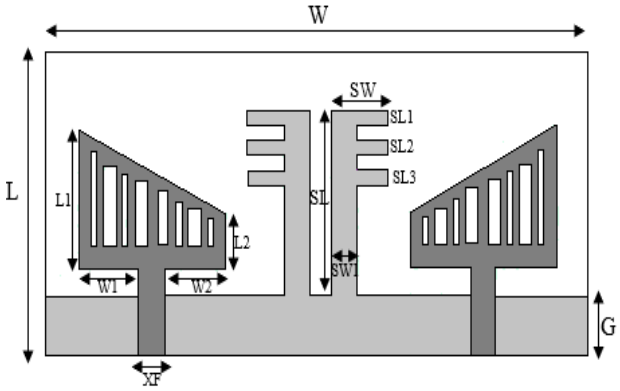

Fig. 1 UWB MIMO Antenna Geometry

Table. 1 Optimized values for dimensions of UWB MIMO antenna.

Parameters	Dimensions (mm)	Parameters	Dimensions (mm)
L	20	XF	3
W	44.1	SL	12.3
L1	9.1	SW	4.5
W1	4.9	SW1	2
L2	3.6	SL1	1
W2	4.9	SL2	1
G	4.47	SL3	1

The circular monopole has been designed using the following relation as:

$$a = \frac{F}{\left\{1 + \frac{2h}{\pi\varepsilon_r F\left[\ln\left(\frac{\pi F}{2h}\right) + 1.7726\right]}\right\}^{1/2}} \quad (1)$$

where $F = \frac{8.791 \times 10^9}{f_r\sqrt{\varepsilon_r}}$

The equations used to calculate the widths of the micro strip feed line are shown below

$$Z_0 = \frac{\eta_0}{2\pi\sqrt{\varepsilon_{re}}} \ln\left\{\frac{F_1}{u} + \sqrt{1 + 4/u^2}\right\} \quad (2)$$

where,

$F_1 = 6 + (2\pi - 6) \times exp\{-(30.666/u)^{0.7528}$

$\eta_0 = 120\pi\Omega$

$u = W/h$ and

$$\varepsilon_{re} = \frac{\varepsilon_r + 1}{2} + \frac{\varepsilon_r - 1}{2}\left(1 + \frac{10}{u}\right)^{-ab} \quad (3)$$

$$b = 0.564\left(\frac{\varepsilon_r - 0.9}{\varepsilon_r + 0.3}\right)^{0.053}$$

$$\frac{W}{h} = \frac{2}{\pi}\left\{B - 1 - ln(2B - 1) + \frac{\varepsilon_r - 1}{2\varepsilon_r}\left[ln(B - 1) + 0.39 - \frac{0.61}{\varepsilon_r}\right]\right\} \quad (4)$$

where,

$$A = \frac{Z_0}{60}\left\{\frac{\varepsilon_r + 1}{2}\right\}^{1/2} + \frac{\varepsilon_r - 1}{\varepsilon_r + 1}\left\{0.23 + \frac{0.11}{\varepsilon_r}\right\}$$

$$B = \frac{60\pi^2}{Z_0\sqrt{\varepsilon_r}}$$

All simulations were performed using High Frequency Simulation Software (HFSS) to validate the provided antenna. Figure 2 depicts the total impact of ground on MIMO antenna bandwidth and impedance of an antenna. Figure 2 shows that antenna bandwidth increases, and impedance is matched at 4.2 mm ground length, which is the offered antenna ground length. In this design, an F-shaped decoupling stub is employed between radiating components to provide good isolation between MIMO antennas. The evaluation steps of without stub and with extended F shaped stub structure for the proposed antenna are depicted in Figure 4. The initial stage is to develop and verified results a plain traditional ground plane. In the second step, an F-shaped stub is attached to the ground plane for customization. The F-shaped stub will provide desirable increased isolation.

Input impedance is directly associated with the return loss. The width parameter of fed point is heavily effective in improving input impedance and, therefore effective aperture of the antenna is increases. This results in the antenna capturing more electromagnetic energy, which leads to higher power reception. Consequently, the reflected power decreases, and the return loss improves. Figure 3 shows proper input impedance is matched at 4.2 mm ground length.

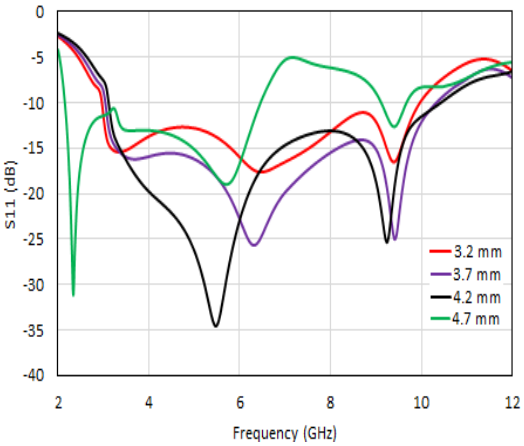

Fig. 2 S-parameters plot for various ground G values

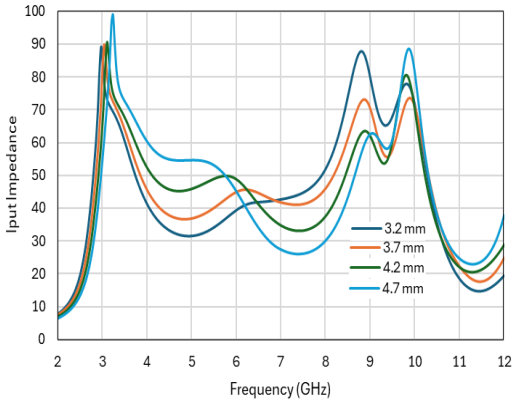

Fig. 3 Distance between the fed points on input impedance

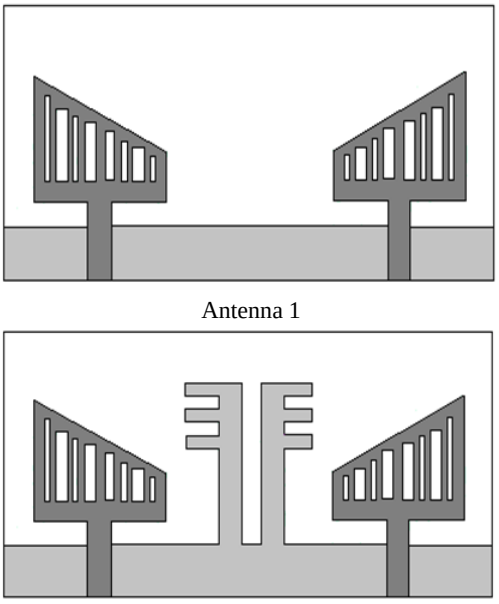

Fig 4 Evaluation of decoupling structure for the proposed MMO antenna.

The two radiating elements and the feed line are designed on the top of the substrate and the ground plane is designed on the bottom of the substrate. The upper

patch is cut by triangular shape and place side by side to achieve wide band matching and good element spacing. Initially a lowered edge stepped cut rectangular shaped UWB patch radiator was designed [20], then modified to triangular shape with two steps cut in the lower edge of the radiator to achieve a wide-band matching." In the first stage a simple triangular shaped radiator was designed and tested for the desired results (Antennab1). Then we were further modified to F-shaped stubs for better MIMO performance (Antenna 2). Fig. 4 shows simulated refection coefficient (S11) and transmission coefficient (S21) of the proposed antenna for simple ground plane and ground plane with F-shaped stubs. It is worth noticing that low mutual coupling is always desirable for high performance MIMO antennas. It can be seen that antenna 1 has poor isolation in the whole UWB range when the conventional ground plane is used. Mutual coupling between the pro-posed antennas is reduced by modifying the ground plane. High isolation between the MIMO antenna elements is achieved by printing F-shaped stubs on the plane.

The traditional ground plane antenna is analysed, and the significant mutual coupling between antenna is -15 dB is obtained in UWB range due to the lack of a decoupling stub. The traditional ground is changed to a F-shaped stub to improve isolation between antennas. Figure 5 depicts the S12 results for antennas with traditional ground plane, and F-shaped stubs. The proposed F-shaped stub provides significantly better performance than the traditional ground plane. The mutual coupling of the proposed antenna is -25 dB for UWB range, as shown in Figure 5. Surface current distributions at various frequencies are shown in Figure 6 for analysis of the proposed antenna. Surface current distributions at various frequencies are shown in Figure 6 for analysis of the proposed antenna.

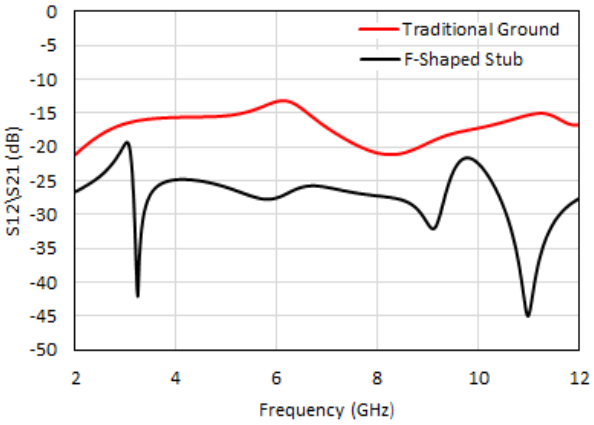

Fig. 5 S12/S21 parameters plot for traditional ground and extended F shaped stub structure.

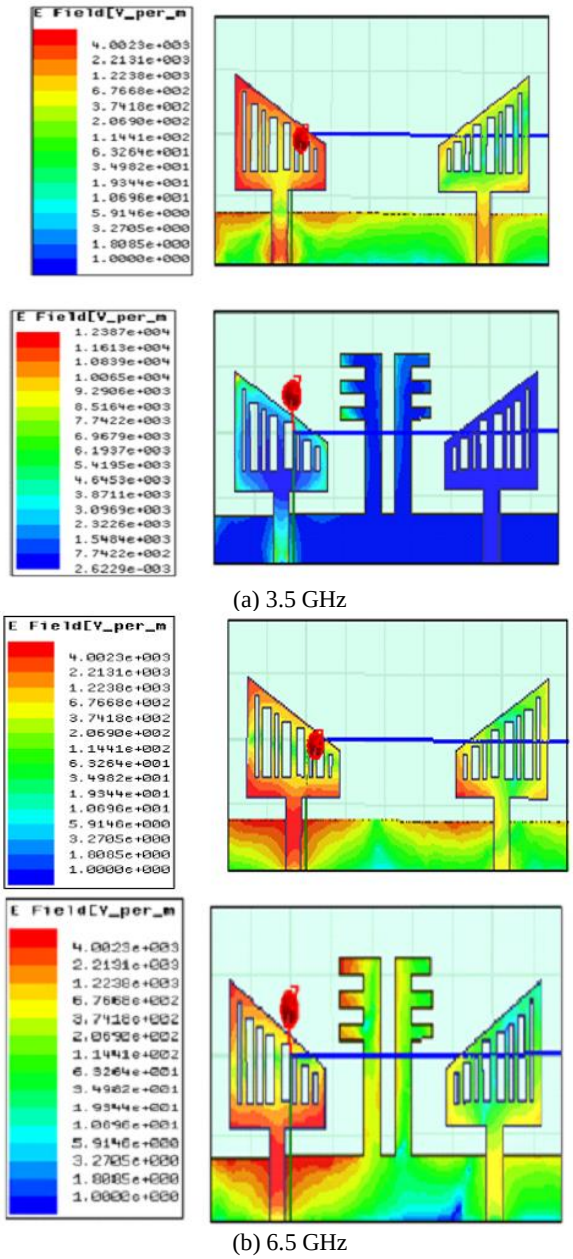

Fig. 6 Surface current distribution for traditional ground and extended F shaped stub structure for different frequencies (a) 3.5 GHz (b) 6.5 GHz.

The performance of proposed antenna is evaluated at 3.5 GHz and 6.5 GHz frequencies activation of port 1. The antenna that is being shown has its port 2 terminated. Figure 6 shows that a large surface current is collected between the two ports in the traditional ground plane, leading to a poor isolation between the two components. An F-shaped decoupling structure is placed between the radiating components to manage the surface current. After installing the F-shaped decoupling structure, the majority of the surface current concentrates at port 1, whereas the coupled current to port 2 is minimised. As a result, optimum isolation between the

two radiating part is achieved. It is important to consider that improved isolation between the radiating elements is always preferable.

3 Antenna Results and Discussion

The proposed antenna structure is made on FR4 substrate and has a 1.6 mm height. It has a 4.4 dielectric constant and a 0.02 loss tangent. The proposed antenna simulated by a HFSS software. Front view and back view of fabricated antenna are shown in Figure 7.

(a) Front view (b) Back view

Fig. 7 Photograph of the proposed antenna: (a) Front view (b) Back view

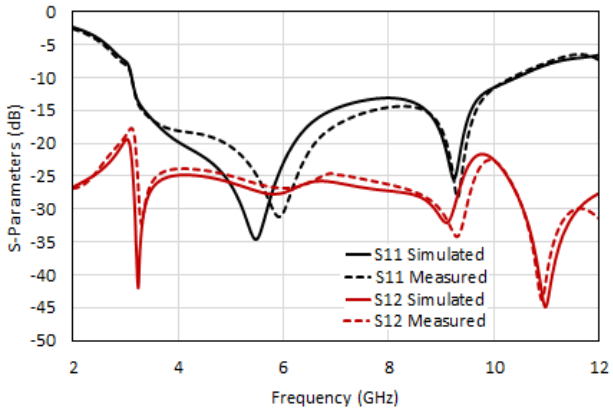

Fig. 8 Measured and simulated reflection Coefficient of proposed MIMO antenna.

Reflection coefficient results are tested using Agilent Network Analyzer (VNA). Figure 8 shows the measured and simulated reflection coefficients of the proposed antenna. $S11 \leq -10$ dB is obtained from 3.1 to 10.6 GHz and $S12 < -25$ dB is achieved from 3.1 to 9.3 GHz. The measured results are good agreement with the simulated results. The minor variations are caused by fabrication material and connector losses. Figure 9 depicts the radiation patterns E-plane and H-plane (co-polar and cross polar) at 3.5 and 6.5 GHz frequencies of the MIMO antenna. One port excited at a time and port 2 is terminated. The radiation patterns at 'port 1' are nearly identical to those at 'port 2', confirming antenna diversity. The proposed antenna has stable radiation pattern at both the frequencies with less cross polarization level.

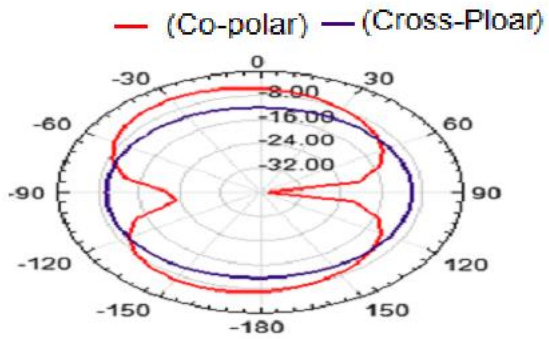

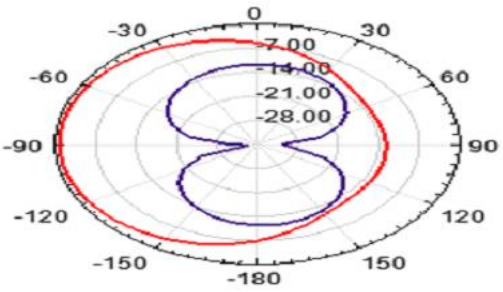

(a) E & H plane

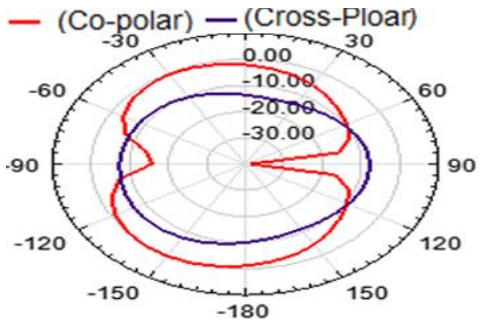

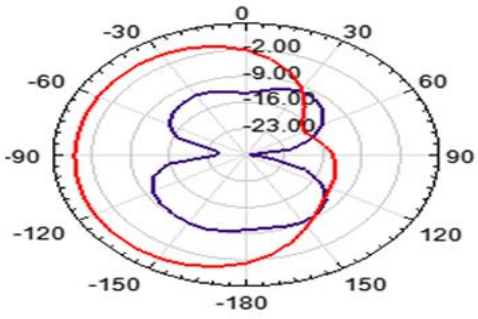

(b) E & H Plane

Fig. 9 Radiation patterns of proposed antenna after decoupling stub (a) 3.5 GHz (b) 6.5 GHz

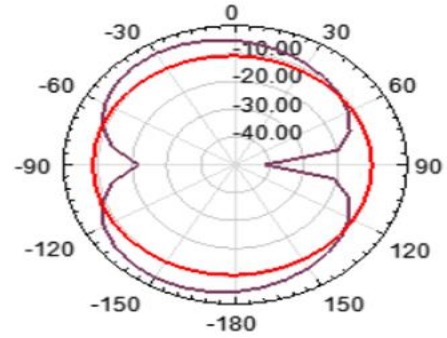

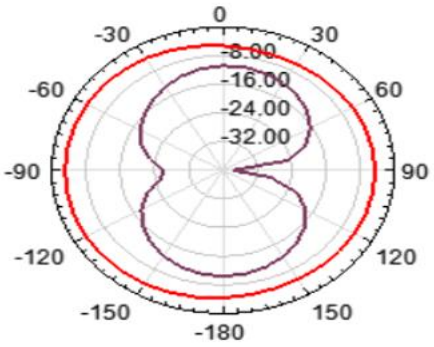

(a) E & H plane

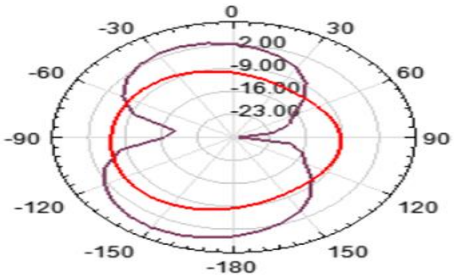

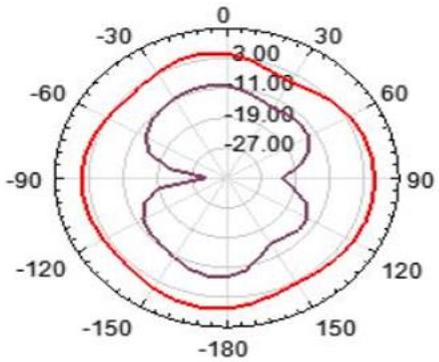

(b) E & H plane

Fig.10 Radiation patterns of proposed antenna before decoupling stub (a) 3.5 GHz (b) 6.5 GHz

Co-polarization and cross-polarization results before decoupling is shown in Fig. 10. The co-pole results are almost Omni directional and stable for both radiators, while the results of the cross-pole are maximum.

The maximum gain of proposed antenna is from 1 dB to 9.3 dB as demonstrated in Figure 11. Gain of an antenna rises exponentially across the entire UWB band. Gain rises as frequency rises. Since the patch size increase with frequency, the gain increases. It is because at a higher frequency the patch dimensions become larger than the corresponding wavelength which results in the enhancement of gain. The diversity performance of the presented MIMO antenna is evaluated by computing diversity parameters such as ECC, DG, and mean effective gain (MEG).

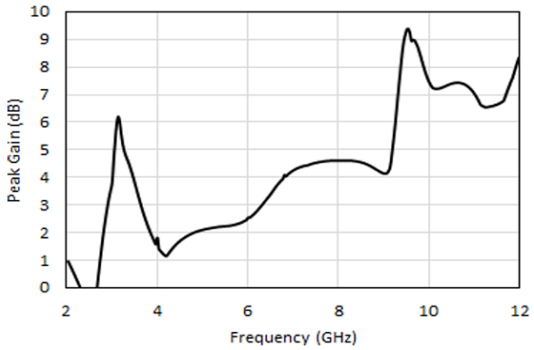

Fig. 11 Gain of the Proposed antenna.

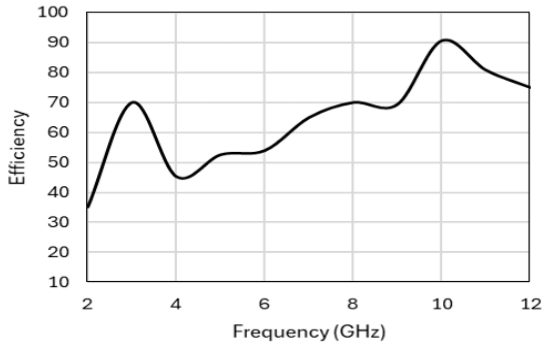

Fig. 12 Radiation Efficiency of proposed antenna

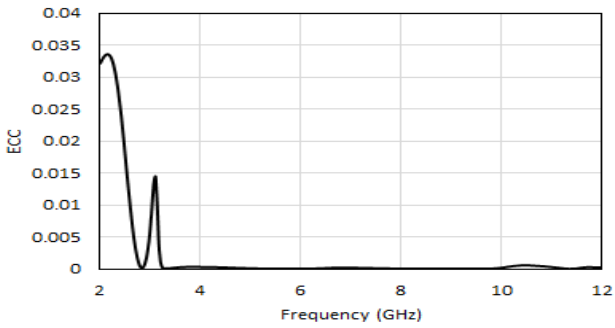

Fig. 13 ECC of the proposed antenna

The proposed antenna efficiency is greater than 40% to 89% in the UWB range as clear from Figure 12.

The isolation between communication channels is defined by ECC. It takes into account how the radiation patterns of the two antennas interact while they are operating simultaneously. ECC can be calculated using equation (5) [19]. Figure 13 shows that the ECC of the presented antenna is less than 0.015 for the frequency range of 3.0 to 12 GHz. The low ECC value indicates

that the antenna offers good performance in terms of diversity.

$$ECC = \frac{|S^*_{11}S_{12} + S^*_{21}S_{22}|}{(1 - |S_{11}|^2 - |S_{21}|^2)\,(1 - |S_{22}|^2 - |S_{12}|^2} \quad (5)$$

The diversity gain (DG) is calculated from the correlation coefficient using equation number (6) [19]

$$DG = 10 \times \sqrt{1 - |\rho|} \quad (6)$$

Where, ρ is the ECC. The diversity gain is 10 dB over the 3.1 GHz to 12 GHz frequency range, showing that the antenna has high diversity performance. MIMO antenna diversity efficiency can be analysed from the Eq. 2 in terms of diversity gain. It is obvious that greater diversity gain is given by the lower value of correlation coefficient. The correlation coefficient is zero in the ideal case and in such ideal case diversity gain is constant with a value of 10. The diversity gain of the proposed UWB-MIMO antenna is shown in Fig. 14.

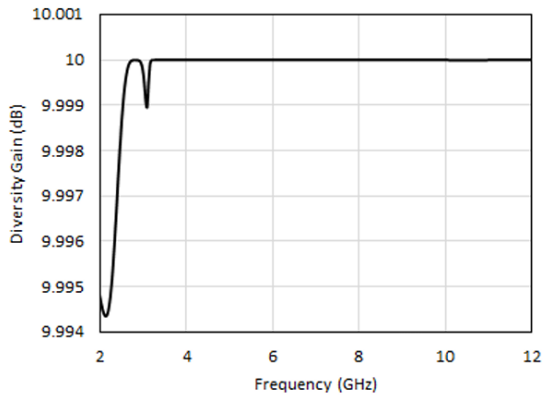

Fig. 14 Diversity Gain of the proposed antenna

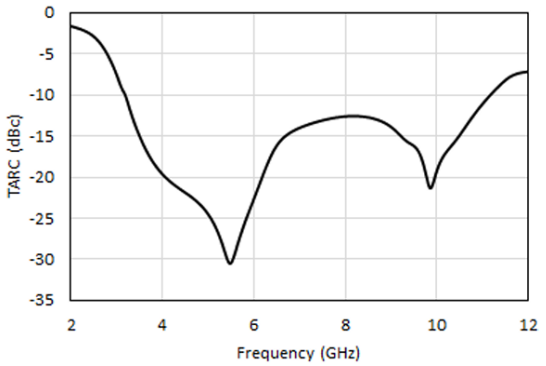

Fig. 15 TARC of the proposed antenna

TARC is defined in (7), where ai and bi are the incident and reflected signals, respectively.

$$\Gamma = \sqrt{\sum_{i=1}^{N}|b_i|^2}/\sqrt{\sum_{i=1}^{N}|a_i|^2} \quad \text{for } \vec{b} = Sp\vec{a} \quad (7)$$

S is the scattering matrix.

To evaluate the MIMO efficiency of the antenna, the total active reflection coefficient (TARC) is taken into account. The exact effect of the mutual coupling on the antenna is assumed TARC (Γ) is calculated using equation (8) and depicted in Figure 15. "Theta is variable range is 0 to 2pi. Theta is angle of observation"

$$\text{TARC} = \frac{\sqrt{\left(\left|S_{11}+S_{12}e^{j\theta}\right|\right)^2\left(\left|S_{21}+S_{22}e^{j\theta}\right|\right)^2}}{\sqrt{2}} \quad (8)$$

The proposed antenna is compared with the previously presented antennas in term of size, bandwidth, isolation, gain and ECC in table 2. The antenna structures in [9-15] are larger in size than our proposed antenna. In [16-17], antenna size is small, but isolation is and gain minimal. Presented antenna is simple to design, easy to fabricate, high gain, and high isolation. It has stable radiation pattern and satisfies all diversity parameters and MIMO requirements.

Table. 2 Comparison of the proposed antenna with antennas in literature.

Ref. #	Size (mm^2)	Band width (GHz)	Isolation (dB)	Gain (dB)	ECC
9	38.5 × 38.5	3.1–10.6	-15	1.4–3.6	0.02
10	40 × 80	4.5–8	-25	2–4	0.002
11	68 × 35	3.1–10.6	-20	1.7–4.2	0.002
12	40 × 20	3-11	-15	2–5	0.3
13	50 × 30	2.5–14.5	-20	0.3–4.3	0.04
14	45 × 25	3.1-12	-15	4.5	0.2
15	36 × 45	3.01-12.5	-20	4-8.24	0.025
16	24 × 32	3.1–12.5	−16	1-4.8	0.05
17	26 × 28	2.9–10.8	-15	1-4	0.5
18	40 × 40	3.1–11	-20	3.28	0.002
21	26x28	4.95	-17	10.6	0.002
22	55.1 × 52.9	9.92-10.8	-35	13.5	0.002
Proposed	20 × 44.1	3.1 to 10.6	-25	1-9.3	0.015

4 Conclusions

In this work, a novel compact high isolation UWB MIMO antenna is presented. The size of antenna is 20 × 44.1 × 1.6 mm^3, however the isolation is enhanced by using a extended F shape decoupling stub. Isolation of an antenna is < -25 dB, ECC < 0.015 and peak gain varies from 1 to 9 dB over 3.1 to 10.6 GHz frequency band. The results of measurement and simulation are in good agreement. The antenna is simple to design, easy to fabricate and low cost. It offers stable radiation patterns and all diversity parameters peak gain, ECC, DG, TRAC are satisfying therefore proposed antenna can be used for

MIMO UWB wireless applications.

References

[1] Federal Communication Commission, "First report and order revision of Part 15 of the Commission's rules regarding ultra-wideband transmission system," Washington, DC, USA, 2002.

[2] Ren, J.; Hu, W.; Yin, Y.; Fan, R. "Compact printed MIMO antenna for UWB applications," IEEE Antennas Wireless Propagation Letter, vol 13, pp. 1517-1520, 2014

[3] Zhang, Z., Wang, X., Long, K., Vasilakos, A. V., & Hanzo, L. "Large-scale MIMO-based wireless backhaul in 5G networks," IEEE Wireless Communications, vol 22 (5), pp. 58-66, 2015

[4] Zhang, J. Y., F. Zhang, W. P. Tian, and Y. L. Luo, "ACS-fed UWB-MIMO antenna with shared radiator," Electronics Letters, vol. 51, no. 17, pp. 1301–1302, 2015.

[5] Roshna, T. K., U. Deepak, V. R. Sajitha, K. Vasudeven, and P. Mohan, "A compact UWB MIMO antenna with reflector to enhance isolation," IEEE Transactions on Antennas and Propagation, vol. 63, no. 4, pp. 1873–1877, 2015.

[6] Azim, R., M. T. Islam, and N. Misran, "Compact tapered-shape slot antenna for UWB applications," IEEE Antennas and Wireless Propagation Letters, vol. 10, pp. 1190–1193, 2011.

[7] Dikmen, C. M., S. Cimen, and G. C, Cakir, "Planar octagonal-shaped uwb antenna with reduced radar cross section," IEEE Transactions on Antennas and Propagation, vol. 62, no. 6, pp. 2946–2953, 2014.

[8] Alsath, M. G. N. and M. Kanagsabai, "Compact UWB monopole antenna for automotive communications," IEEE Transactions on Antennas and Propagation, vol. 63, no. 9, pp. 4204–4208, 2015.

[9] Kang, L., H. Li, X. Wang, and X. Shi, "Compact offset microstrip-fed MIMO antenna for band notched UWB applications," IEEE Antennas and Wireless Propagation Letters, vol. 14, pp. 1754–1757, 2015.

[10] Jabire, A.H.; Zheng, H.X.; Abdu, A.; Song, Z. "Characteristic mode analysis and design of wide band MIMO antenna consisting of metamaterial unit cell," Electronics, vol. 8, pp. 68, 2019.

[11] Li, W.T.; Hei, Y.Q.; Subbaraman, H.; Shi, X.W.; Chen, R.T. "Novel printed filtenna with dual notches and good out-of-band characteristics for UWB-MIMO applications," IEEE Microwave Wireless Component Letter, vol. 26, pp. 765–767, 2016.

[12] Mathur, R. and S. Dwari, "Compact planar reconfigurable UWB-MIMO antenna with on demand worldwide interoperability for microwave access wireless local area network rejection," IET Microwaves, Antennas & Propagation, vol. 13, no. 10, pp. 1684–1689, 2019.

[13] Iqbal, A.; Saraereh, O.A.; Ahmad, A.W.; Bashir, S. "Mutual coupling reduction using F-shaped stubs in UWB-MIMO antenna," IEEE Access, vol. 6, pp. 2755–2759, 2017.

[14] Mathur, R. and S. Dwari, "Compact CPW-fed ultrawideband MIMO antenna using hexagonal ring monopole antenna elements," AEU International Journal of Electronics and Communications, vol. 93, pp. 1–6, 2018.

[15] Srivastava, K.; Kumar, A.; Kanaujia, B.K.; Dwari, S.; Kumar, S. "A CPW-fed UWB MIMO antenna with integrated GSM band and dual band notches," International Journal RF Microwave Computer Aided Engineering, vol. 29, e21433, 2019

[16] Gurjar, R.; Upadhyay, D.K.; Kanaujia, B.K.; Sharma, K. "A novel compact self-similar fractal UWB MIMO antenna," International Journal RF Microwave Computer Aided Engineering, vol. 29, e21632, 2019.

[17] Zhao, Y.; Zhang, F.S.; Cao, L.X.; Li, D.H. A Compact Dual Band-Notched MIMO Diversity Antenna for UWB Wireless Applications. Progress in Electromagnetic Research, vol. 89, pp. 161–169, 2019.

[18] Ali, W.A.; Ibrahim, A.A. A compact double-sided MIMO antenna with an improved isolation for UWB applications. AEU International Journal of Electronics and Communications, vol. 82, pp. 7–13, 2017

[19] A Khade, M. A. Trimukhe, SM Verulkar, RK Gupta "Dual Band MIMO Antenna with High Isolation for GSM and WLAN Applications," Progress in Electromagnetics Research C, vol. 136, pp. 189-198, 2023.

[20] A. Iqbal, O. A. Saraereh, and S. K. Jaiswal, "Maple leaf shaped UWB monopole antenna with dual band notch functionality," Progress in Electromagnetics Research C, vol. 71, pp. 169-175, Feb. 2017.

[21] Hamed Nimehvari Varcheh, "Integration of the modified Butler matrix and decoupling network for beam-steering antenna array," International Journal of RF and Microwave Computer-Aided Engineering, Vol.32, Dec. 2021.

[22] A. A. Diman et al., "Efficient SIW-Feed Network Suppressing Mutual Coupling of Slot Antenna Array," in IEEE Transactions on Antennas and Propagation, vol. 69, no. 9, pp. 6058-6063, Sept. 2021

[23] C. Balanis. Antenna theory, analysis and design, 2nd ed. JohnWiley & Sons, Inc, 2009.
[24] Kumar, R. and S. Gaikwad, “On the design of nano-arm fractal antenna for UWB wireless applications,” Journal of Microwaves, Optoelectronics and Electromagnetic Applications, Vol.12 No.1,158-171 2013.